Cellular/Molecular

Neurexin-β Mediates the Synaptogenic Activity of Amyloid Precursor Protein

Vedrana Cvetkovska,[1*] Yuan Ge,[1*] Qin Xu,[2] Shaokun Li,[2] Peng Zhang,[1,2] and Ann Marie Craig[1]

[1]Djavad Mowafaghian Centre for Brain Health and Department of Psychiatry, University of British Columbia, Vancouver, British Columbia V6T 2B5, Canada and [2]Department of Neurosciences, School of Medicine, Case Western Reserve University, Cleveland, Ohio 44106

In addition to its role in Alzheimer's disease, amyloid precursor protein (APP) has physiological roles in synapse development and function. APP induces presynaptic differentiation when presented to axons, but the mechanism is unknown. Here we show that APP binds neurexin to mediate this synaptogenic activity. APP specifically binds β not α neurexins modulated by splice site 4. Binding to neurexin heparan sulfate glycan and LNS protein domains is required for high-affinity interaction and for full-length APP to recruit axonal neurexin. The synaptogenic activity of APP is abolished by triple knockdown of neurexins in hippocampal neurons pooled from male and female rats. Based on these and previous results, our model is that a dendritic-axonal *trans* dimer of full-length APP binds to axonal neurexin-β to promote synaptic differentiation and function. Furthermore, soluble sAPPs also bind neurexin-β and inhibit its interaction with neuroligin-1, raising the possibility that disruption of neurexin function by altered levels of full-length APP and its cleavage products may contribute to early synaptic deficits in Alzheimer's disease.

Key words: **Alzheimer's disease; amyloid precursor protein; neurexin; presynaptic; synaptic organizing protein; synaptogenesis**

Significance Statement

The prevailing model for the basis of Alzheimer's disease is the amyloid cascade triggered by altered cleavage of amyloid precursor protein (APP). APP also has physiological roles at the synapse, but the molecular basis for its synaptic functions is not well understood. Here, we show that APP binds the presynaptic organizing protein neurexin-β and that neurexin is essential for the synaptogenic activity of APP. Furthermore, soluble APP forms generated by APP cleavage also bind neurexin-β and can block interaction with transmembrane synaptogenic ligands of neurexin. These findings reveal a role for neurexin-APP interaction in synapse development and raise the possibility that disruptions of neurexin function may contribute to synaptic and cognitive deficits in the critical early stage of Alzheimer's disease.

Introduction

APP is a conserved transmembrane protein that is extensively cleaved by α-, β-, and γ-secretases creating numerous cleavage products, including Aβ involved in Alzheimer's disease (AD) pathogenesis (Selkoe and Hardy, 2016). Aβ impairs synaptic structure and function (Canter et al., 2016), and a recent study found that reduction of glutamatergic synaptic transmission and plasticity by Aβ oligomers depends on native APP (Rolland et al., 2020). Synaptic loss is widely accepted to be an early step in AD pathogenesis, and a meta-analysis revealed selective vulnerability of presynaptic components (de Wilde et al., 2016). In contrast to the detrimental effects of Aβ, numerous studies support physiological roles for full-length APP in promoting synapse development and function (for review, see Muller et al., 2017), including in triggering presynaptic differentiation (Wang et al., 2009). Thus, perturbed synaptic organizing activity by full-length APP as well as toxic effects of Aβ may contribute to synaptic dysfunction in AD.

In the mammalian neuromuscular junction, APP is required in both cholinergic neurons and target muscles for correct synaptic differentiation (Wang et al., 2009). As APP is present both in presynaptic and postsynaptic compartments, some studies have suggested that a trans-synaptic APP dimer participates in synapse formation and stabilization (Wang et al., 2009; Baumkotter et al., 2014).

Received Mar. 10, 2021; revised Sep. 13, 2022; accepted Oct. 12, 2022.

Author contributions: V.C., Y.G., P.Z. and A.M.C. designed research, V.C., Y.G., Q.X., S.L., and P.Z. performed research, V.C., Y.G., Q.X., S.L., P.Z., and A.M.C. analyzed data, V.C. and A.M.C. wrote the paper, Y.G. and P.Z. edited the paper.

This work was supported by Michael Smith Foundation for Health Research/Pacific Alzheimer Research Foundation Postdoctoral Fellowship Award to V.C.; Canadian Institutes for Health Research Grant FDN-143206 and Canada Research Chair Award to A.M.C.; and SFARI Bridge to Independence Award to P.Z. We thank Xiling Zhou for assistance with neuron cultures.

*V.C. and Y.G contributed equally to this work.

V. Cvetkovska's present address: Department of Psychology, McGill University, Montreal, QC, H3A 1B1, Canada.

The authors declare no competing financial interests.

Correspondence should be addressed to Ann Marie Craig at acraig@mail.ubc.ca.

https://doi.org/10.1523/JNEUROSCI.0511-21.2022

Dimers involved may include APP with itself and the closely related Amyloid Precursor-Like Proteins (Wang et al., 2009; Schilling et al., 2017). A powerful demonstration of the synapse-promoting role of APP is the finding that presentation of APP to axons is sufficient to trigger local presynaptic differentiation (Wang et al., 2009). This synaptogenic activity requires axonal APP family members, APP dimerization, copper binding to APP, and is reduced by APP cleavage (Wang et al., 2009; Baumkotter et al., 2014; Stahl et al., 2014). A proteomics screen revealed close interactions of APP with synaptotagmin-1 and synaptic vesicle proteins (Kohli et al., 2012), and APP and its soluble ectodomain forms modulate transmission through presynaptic $GABA_B$ receptors (Rice et al., 2019). Yet the signal transduction mechanism through which APP triggers presynaptic differentiation is unknown.

Recently, Aβ oligomers were found to interact with neurexins (Nrxs) and modulate their function (Naito et al., 2017). Nrxs are presynaptic organizer protein hubs that recruit extensive protein machinery involved in the differentiation, maintenance, and function of synapses (Reissner et al., 2013; Sudhof, 2017; Gomez et al., 2021). Nrxs interact with several families of postsynaptic ligands, including the neuroligins (NLs), LRRTMs, and cerebellin-GluD complexes (Jeong et al., 2017; Roppongi et al., 2017; Sudhof, 2017; Yuzaki, 2018). The three mammalian Nrx genes show partial overlap in expression and function. While mice survive deletion of any one but not all three Nrx genes (Missler et al., 2003), loss of individual Nrx genes perturbs synaptic transmission in specific circuits (e.g., Aoto et al., 2015). Further molecular diversity generated from each Nrx gene by transcription at two alternate promoters producing long Nrx-α and short Nrx-β forms and alternative splicing at up to six splice sites regulates ligand interactions and function (Gomez et al., 2021). Nrx function is also regulated by post-translational modifications. In particular, heparan sulfate (HS) modification is necessary for the function of all Nrxs by participating in the binding interface for NLs and LRRTMs (Zhang et al., 2018).

Here we show that APP interacts with all Nrx-β in a manner similar to that of Nrx's other synaptogenic ligands, through dual HS and protein domain binding, involving a higher-affinity interaction distinct from that of Aβ oligomers. Furthermore, the synaptogenic activity of APP requires axonal Nrxs. Perturbations of APP-Nrx interactions may contribute to synaptic dysfunction in neurologic disorders, including the early, subtle synaptic changes that occur in the preclinical stages of AD.

Materials and Methods

DNA constructs. Plasmids were generated using standard restriction enzyme cloning or Gibson assembly (NEB). V5-tagged Nrx mouse cDNA constructs (Zhang et al., 2018) were subcloned into a pCAGGS vector between EcoRI and PacI for COS-7 expression. The extracellular domain of V5-Nrx1β (amino acids 1-358) was subcloned into a pHLsec-Avi3-His vector (Aricescu et al., 2006) between EcoRI and KpnI for protein purification in HEK293 cells. Neural expression of Nrx1β was done with pLL3.7hSyn-YFP-2A-V5-Nrx1β WT or ΔHS mutant (Zhang et al., 2018). Nrx deletion mutants were described previously (Graf et al., 2004).

The Nrx triple-knockdown (shNrx) adeno-associated virus (AAV) vector pAAV-rNrx-TKD was made by subcloning the whole four shRNA cassettes from previous pFB-AAV-rNrx-TKD (Zhang et al., 2018) into the BglII and XhoI sites of pAAV.hSyn.eGFP.WPRE.bGH vector (Addgene #105539) for viral packaging in a mammalian cell line. An shRNA against MorB (Takahashi et al., 2011) was inserted into the same pAAV backbone to generate pAAV-U6-shMorB-hSyn-Cre as a control (shCon). shMorB was chosen as a control because it was previously found to have no effect on neuron morphology and did not activate interferon target genes (Alvarez et al., 2006).

All APP constructs were derived from human APP695 cDNA and subcloned into a pCAGGS vector between EcoRI and KpnI with an Myc tag added at the mature N-terminus to facilitate detection. Noncleavable APP* was generated by deleting amino acid residues 592-621. The dimerization mutant APP* $GFLD^{mut}$ was generated by mutating histidine at residues 108 and 110 to alanines as reported (Baumkotter et al., 2014). The APP* E1-RA mutant was generated by mutating amino acid residues 99-102 from KRGR to AAAA. The APP* E2-RA mutant was generated by mutating amino acid residues 327-330 from HRER to AAAA. The APP* RA mutant refers to a dual E1 and E2 mutant containing both mutations above, 99-102 KRGR to AAAA and 327-330 HRER to AAAA.

Myc-CD4 was created by replacing the HA tag in HA-CD4 (Pettem et al., 2013) with an Myc tag. Other plasmids have been described previously: HA-NL2 (Scheiffele et al., 2000), HA-NGL-3 (Bomkamp et al., 2019), and pcDNA4-HA-ecto-NL1-His (Zhang et al., 2018).

Antibodies. The following primary antibodies were used: mouse monoclonal anti-APP (1:1000, IgG1, clone 6E10, BioLegend), mouse monoclonal anti-V5 (1:5000; IgG2a, Thermo Fisher Scientific), rabbit polyclonal anti-Myc (1:7000, Sigma Aldrich), mouse monoclonal anti-Myc (1:5000; IgG1, clone 9E10, Santa Cruz Biotechnology), mouse monoclonal anti-HA (1:1000, IgG2b, clone 12CA5, Roche), rat monoclonal anti-HA (1:1000, clone 3F10, Roche), mouse monoclonal anti-synapsin1 (1:8000, IgG1, clone 46.1, Synaptic Systems), rabbit polyclonal anti-synapsin1 (1:2000, Millipore), mouse monoclonal anti-vGluT1 (1:4000, IgG1, clone N28/9, NeuroMab), guinea pig polyclonal anti-vGAT (1:3000; Millipore), mouse monoclonal anti-tau1 (1:4000, IgG2a, clone PC1C6, Millipore), chicken polyclonal anti-MAP2 (1:8000; Abcam), rabbit polyclonal anti-GFP (1:20,000; Thermo Fisher Scientific Scientific), and mouse monoclonal anti-His (1:1000, IgG2b, clone HIS.H8, Thermo Fisher Scientific).

The following secondary antibodies were used: highly cross-adsorbed, goat Alexa dye-conjugated secondary antibodies toward the appropriate species and monoclonal isotype (1:1000; Thermo Fisher Scientific; Alexa-488, Alexa-568, and Alexa-647 labeled secondary antibodies) and AMCA-conjugated anti-chicken IgY (donkey IgG; 1:400; Jackson ImmunoResearch Laboratories). For the replication of the sAPPα and sAPPβ binding curves, biotin-SP-conjugated anti-mouse Fc fragment (IgG2b; 1:1000; Jackson ImmunoResearch Laboratories) and Alexa-568-conjugated Streptavidin (1:1000; Invitrogen) were used to detect anti-His antibody. For the binding competition experiment, Alexa-594-conjugated anti-human Fc fragment (goat; 1:500; Jackson ImmunoResearch Laboratories) was used to detect bound ecto-NL1-Fc.

AAV production. AAV production was done as previously described (Niemi et al., 2016). In brief, pAAV-rNrx-TKD or pAAV-U6-shMorB-hSyn-Cre was cotransfected with pUCmini-iCAP-PHP-cB (Addgene #103005) and pADDeltaF6 (gift from Richard Zigmond, originally from Addgene #112867) plasmids in a ratio of 1:4:2 into HEK293FT cells. Cells were cultured in DMEM with 10% FBS for 16 h and then in DMEM with 3% FBS for 72 h. The cells were treated with benzonase nuclease to release the recombinant AAV particles. The resulting mixture was pooled with condition medium to increase the total yield. The AAV particles were concentrated by PEG8000 precipitation, chloroform extraction, then centrifugation with an Amicon Ultra-50 filter.

Cell culture, transfection, AAV transduction. Low-density primary hippocampal cultures were prepared from E18 rat embryos from both sexes as previously described (Kaech and Banker, 2006). Neuron cultures were maintained in Neurobasal medium (Thermo Fisher Scientific) supplemented with GlutaMAX-I (Thermo Fisher Scientific), B-27 supplement (Thermo Fisher Scientific). COS-7 cells were cultured in DMEM supplemented with 10% bovine growth serum and 100 IU/ml penicillin-streptomycin.

COS-7 cells were transfected using TransIT-LT1 transfection reagent (Mirus Bio) or Lipofectamine 2000 (Thermo Fisher Scientific). For neural expression of plasmids, one million primary hippocampal neurons were transfected at DIV 0 using nucleofection (AMAXA Biosystems, Lonza). Neurons were treated with cytosine arabinoside at DIV 2, and then with 100 mM DL-2-amino-5-phosphonovaleric acid

(APV) beginning on DIV 7 to limit excitotoxicity. For AAV-mediated knockdown experiments, low-density hippocampal cultures growing on coverslips were exposed to recombinant AAV viral vector particles for 4 h at DIV 3 and then returned to their home dishes.

Western blot. For confirmation of Nrx triple knockdown, AAV-treated primary hippocampal neuron cultures were scraped from coverslips and incubated with or without 1 U/ml each of heparinases I, II, and III for 2 h at 37°C in the buffer: 20 mM Tris-HCl, pH 7, 100 mM NaCl, 1.5 mM $CaCl_2$, EDTA-free protease inhibitor cocktail. The resulting samples were dissolved in SDS-loading buffer and subjected to an SDS-polyacrylamide gel (prepared using TGX FastCast Acrylamide Kit, 7.5%; Bio-Rad) electrophoresis and were transferred to Immobilon P membranes (Millipore). The membrane was blocked with 5% milk for 1 h at room temperature, immunoblotted with primary antibodies overnight at 4°C, and then incubated with HRP-conjugated secondary antibodies (1:10 000, Southern Biotechnology) for 1 h at room temperature. Blots were developed using the Immobilon Western Chemiluminescent HRP Substrate kit (Millipore) and imaged with the Bio Rad gel imaging system. Protein band intensities were quantified with Image Lab software (Bio-Rad). The following primary antibodies were used: anti-pan-Neurexin (1:2000; Millipore, ABN161) and anti-α-tubulin (1:10,000; Millipore).

Immunocytochemistry. Neurons, COS-7 cells, or cocultures were fixed for 12 min with warm 4% PFA and 4% sucrose in PBS, pH 7.4. For surface staining, the cells were first blocked in blocking buffer (3% BSA, 5% normal goat serum in PBS) for 30 min at 37°C and then incubated with primary antibodies, then permeabilized with 0.2% Triton X-100 for 5 min followed by a second incubation with blocking buffer for 30 min at 37°C. For labeling nonsurface proteins, the cultures were then incubated with primary antibodies overnight at 4°C. Incubation with secondary antibodies was done the following day for 30 min at 37°C, and the coverslips were mounted onto slides using elvanol (Tris-HCl, glycerol, and polyvinyl alcohol with 2% 1,4-diazabi-cyclo[2,2,2]octane).

Protein binding assays. Soluble recombinant APP fragments, His-tagged sAPPα and sAPPβ, were purchased from Sigma Aldrich. Soluble V5-Nrx1β ectodomain was generated by transfecting HEK293T cells with pHLsec-ecto-V5-Nrx1β-Avi3-His and collecting the conditioned medium over 48 h. Soluble HA-ecto-NL1-His protein was generated by transfecting HEK293T cells with pcDNA4-HA-ecto-NL1-His and collecting the culture media over 48 h. The recombinant proteins were concentrated using a Centricon Plus-70 centrifugal filter with a 30 kDa cutoff (Millipore) and purified by the His tag with Ni-NTA agarose beads (QIAGEN). Soluble ecto-NL1-Fc protein was produced from HEK293T cells stably expressing the encoding plasmid through Zeocin-based selection, as described previously (Pettem et al., 2013). The conditioned medium was collected every 2-3 d for 3 weeks, and concentrated using a Centricon Plus-70 centrifugal filter with a 30 kDa cutoff (Millipore). The Fc fusion proteins were purified by binding to protein G beads (GE Healthcare).

Binding curves for sAPPα and sAPPβ were generated by incubating COS-7 cells transfected with V5-Nrx1β(–S4) with increasing concentrations of soluble APP (0-200 nM) diluted in binding buffer (168 mM NaCl, 2.6 mM KCl, 10 mM HEPES, pH 7.2, 2 mM $CaCl_2$, 2 mM $MgCl_2$, 10 mM D-glucose, and 100 μg/ml BSA) for 1 h at 4°C. The cells were washed with binding buffer, fixed, and expressed Nrx, and bound soluble APPs were detected with antibodies against the V5 and His tags.

The binding of V5-Nrx1β ectodomain (100 nM) to Myc tagged APP*, APP* $GFLD^{mut}$, or CD4 expressed in COS-7 cells was performed in the same binding buffer. Cell surface-expressed proteins were detected with the Myc tag and bound Nrx1β ectodomain with the V5 tag.

Other binding experiments were performed with sAPPα diluted to 100 nM (see Figs. 1*A*,*B* and 3*C*,*D*) or 6 or 50 nM (see Fig. 4*A*,*B*,*E*,*F*) in binding buffer. Bound sAPPα was detected with the anti-APP antibody. For the binding competition experiment, COS-7 cells transfected with V5-Nrx1β(–S4) were incubated with 100 nM HA-ecto-NL1-His or ecto-NL1-Fc or with binding buffer for 1 h at 4°C. The cells were washed with binding buffer and then incubated with 6 or 20 nM sAPPα for an additional 1 h at 4°C. Alternatively, the transfected cells were incubated with 100 nM sAPPα or with binding buffer for 1 h at 4°C, washed with binding buffer, and then incubated with 20 nM ecto-NL1-Fc for an additional 1 h at 4°C. The cells were then washed with binding buffer and fixed for subsequent immunostaining.

Coculture assays. Coculture assays were performed essentially as described previously (Zhang et al., 2018). For the neurexin recruitment assay, primary hippocampal neurons were transfected with 2.5 µg pLL3.7hSyn-YFP-2A-V5-Nrx-1β WT or ΔHS constructs (Zhang et al., 2018) at DIV 0 using nucleofection (AMAXA Biosystems, Lonza). COS-7 cells were transfected with 2 µg plasmids Myc-APP*, Myc-APP* RA mutant, or Myc-CD4. COS-7 cells were trypsinized 24 h after transfection and plated onto DIV 14 neurons for 2 d before fixation. Cocultures were fixed for 12 min with warm 4% PFA and 4% sucrose in PBS, pH 7.4, stained for surface V5-Nrx on neurons and Myc-APP* or Myc-CD4 on COS-7 cells. After permeabilization, the cocultures were further incubated with anti-GFP and anti-MAP2 antibodies to visualize transfected cells and dendrites, respectively.

For the hemi-synapse formation assay, COS-7 cells were transfected using Lipofectamine 2000 (Thermo Fisher Scientific) with 2 µg of plasmid. One day after transfection, COS-7 cells were seeded onto 13 DIV hippocampal cultures. After 40-48 h, the cocultures were fixed and processed by immunostaining for combinations of surface Myc-APP*, surface HA-NL2, surface HA-NGL-3, synapsin, vGluT1, vGAT, MAP2, and tau1.

Fluorescence imaging and analysis. Fluorescence microscopy was performed using a Zeiss Axioplan2 microscope or a Zeiss LSM700 laser scanning microscope. All images were acquired with a 40× oil immersion objective (NA 1.4) using MetaMorph or Zeiss Zen Blue imaging software.

Image acquisition and analysis were performed with the experimenter blind to the experimental condition. Analysis was performed using National Institutes of Health's ImageJ software. Sets of cells used for quantification were stained simultaneously and imaged with identical settings. For quantification, cells were selected based on similar expression of the transfected construct. Post-analysis images were adjusted for brightness and contrast across the entire image for presentation.

Binding of APP to transfected cells was reported as the ratio between surface APP signal and surface V5 signal.

Recruitment of V5-Neurexin by COS-7 cells expressing different Myc-tagged proteins was reported as the ratio of integrated intensity of V5 over YFP, per contact area of YFP-positive axons, excluding MAP2-positive dendrite contacts.

Presynaptic induction in coculture experiments was measured as the total integrated intensity of punctate synapsin staining signal on a COS-7 cell normalized to the tau-positive axon contacting area, excluding signal onto MAP2-positive dendrite contacts.

Statistics. Statistical analysis was performed using GraphPad Prism software. All data were checked for normality using D'Agostino and Pearson tests before choosing the appropriate comparison test. For data that passed the normality tests, statistical significance was calculated using the Student's *t* test or one-way ANOVA with *post hoc* Bonferroni multiple comparison. For data that did not pass the normality tests, statistical significance was calculated using the Mann–Whitney *U* test or Kruskal–Wallis test with *post hoc* Dunn's multiple comparison. Statistical significance was set at $p < 0.05$. All data are presented as mean ± SEM.

Results

APP binds with high affinity to Nrx-β but not Nrx-α

To test whether the APP ectodomain binds to Nrx, we used a cell-based binding assay as has been used to show interactions of Nrx with other ligands (Boucard et al., 2005; Chih et al., 2006; Graf et al., 2006; Siddiqui et al., 2010). We expressed Nrx 1, 2, and 3 α and β forms with an extracellular V5 tag on the surface of COS-7 cells and tested binding of recombinant sAPPα, the product of α-secretase corresponding to the APP ectodomain. Indeed, we found that sAPPα bound Nrx (Fig. 1*A*). Compared with neighboring nontransfected cells, significant binding of sAPPα was found to cells expressing all Nrx-β but not Nrx-α

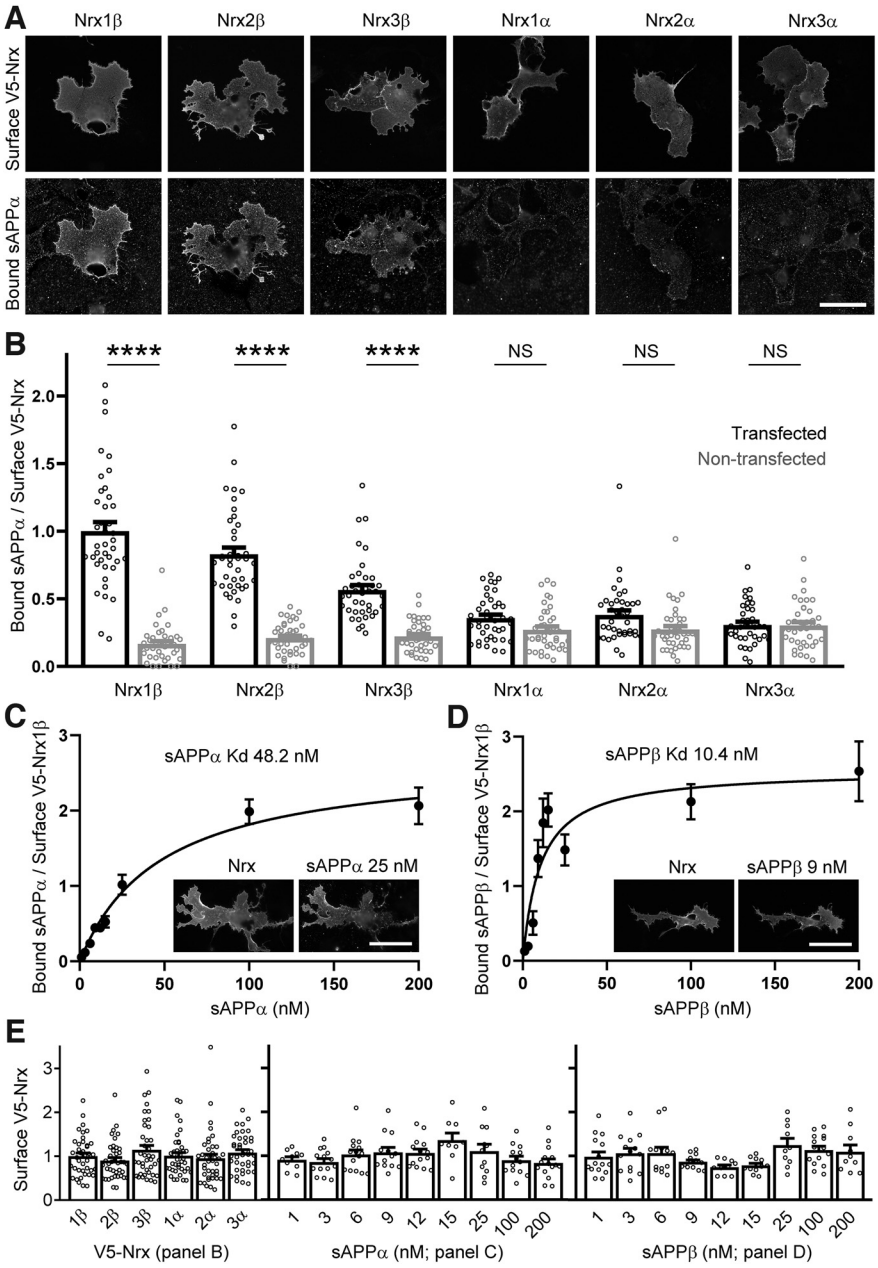

Figure 1. sAPP binds β-Nrx. ***A***, V5-tagged Nrx 1, 2, and 3 β and α forms were expressed in COS-7 cells and incubated with purified sAPPα (100 nM). Cells were immunolabeled for cell surface V5-Nrx and bound sAPPα. ***B***, sAPPα showed significant binding to all β-Nrx but not α-Nrx expressed on COS-7 cells. $p < 0.0001$ (Kruskal–Wallis). ****$p < 0.0001$ or NS not significant, $p = 0.223$ for Nrx1α, $p = 0.107$ for Nrx2α, and $p > 0.999$ for Nrx3α comparing each transfected cell group with neighbouring nontransfected cells (all by Dunn's multiple comparison *post hoc* test) $n = 40$ cells each from three independent experiments. ***C***, ***D***, Scatchard analyses of the COS-7 cell-based binding assay revealed an apparent K_d 48.2 nM for sAPPα with Nrx1β (***C***) and apparent K_d 10.4 nM for sAPPβ with Nrx1β (***D***), $p < 0.0001$ by extra sum-of-squares F test. $n = 9$-15 cells for each data point. An independent replication gave an apparent K_d 57.2 nM for sAPPα and 18.6 nM for sAPPβ with Nrx1β, $p < 0.0001$ by extra sum-of-squares F test. $n = 12$-15 cells for each data point (not shown). Images are shown for surface V5-Nrx1β and bound sAPPα (25 nM concentration) or sAPPβ (9 nM concentration). ***E***, For all of the above binding assays, the COS-7 cells analyzed did not differ in surface expression of V5-Nrx. $p = 0.284$ for the Nrx 1, 2, and 3 β and α forms, $p = 0.119$ for Nrx1β in the sAPPα Scatchard analysis, and $p = 0.056$ for Nrx1β in the sAPPβ Scatchard analysis (all Kruskal–Wallis). Scale bars, 50 μm.

forms (Fig. 1*B*). Scatchard analysis revealed binding in the physiologically significant range with an apparent K_d for sAPPα to Nrx1β of 48.2-57.2 nM in this cell-based assay (Fig. 1*C*). sAPPβ, the product of β-secretase, which is 16 amino acids shorter than sAPPα, also bound Nrx1β with an apparent K_d of 10.4-18.6 nM (Fig. 1*D*, significantly different from sAPPα). For all the binding assays, the cells analyzed did not differ in surface expression of V5-Nrx (Fig. 1*E*). For comparison, in a similar cell-based binding assay, the apparent K_d of NL1 and LRRTM2 ectodomains for Nrx1β was in the range of 9-30 nM (Siddiqui et al., 2010) while the K_d of Aβ oligomers for Nrx1β was 183.5 nM (Naito et al., 2017). Thus, the APP ectodomain binds Nrxβ with an affinity similar to that of postsynaptic ligands and greater than that of Aβ oligomers.

To test whether full-length APP binds the extracellular domain of Nrx1β, we did a cell-based binding assay with the surface-expressed and soluble components reversed. We first generated APPΔ592-621 (called here APP*) incorporating a deletion of the α and β cleavage sites, which eliminates ectodomain cleavage (Stahl et al., 2014) to isolate binding properties of full-length APP and maximize its cell surface expression. Purified V5-tagged Nrx1β ectodomain was used to test binding. Indeed, Nrx1β ectodomain showed significant binding to COS-7 cells expressing APP* compared with background binding to cells expressing CD4 (Fig. 2). To assess whether APP dimerization may play a role in this interaction, we used the mutant APP* H108A/H110A "GFLD^{mut}," which reduces dimerization to ~40% of WT APP level (Baumkotter et al., 2014). This mutation also reduced binding to Nrx1β ectodomain to 63% of WT APP* level (Fig. 2), suggesting that APP dimerization may contribute to its interaction with Nrx1β.

NL1 competes with APP for binding to Nrx1β

The selectivity profile of APP for binding Nrx-β but not Nrx-α is similar to that of another Nrx ligand, the canonical ligand, the major NL1 form containing the B splice insert (Boucard et al., 2005). We thus tested whether NL1 and APP might compete for binding to Nrx1β, via binding to a common or overlapping domain. We expressed Nrx1β on the surface of COS-7 cells and preincubated the cells with soluble NL1 ectodomain before performing a binding assay with sAPPα. Indeed, prebinding of the NL1 ectodomain significantly reduced subsequent sAPPα binding, compared with cells that were pretreated with buffer alone (Fig. 3*A*–*C*). Conversely, preincubation of COS-7 cells expressing Nrx1β with sAPPα significantly reduced subsequent binding of NL1 ectodomain (Fig. 3*D*–*F*), Thus, NL1 and APP compete for binding

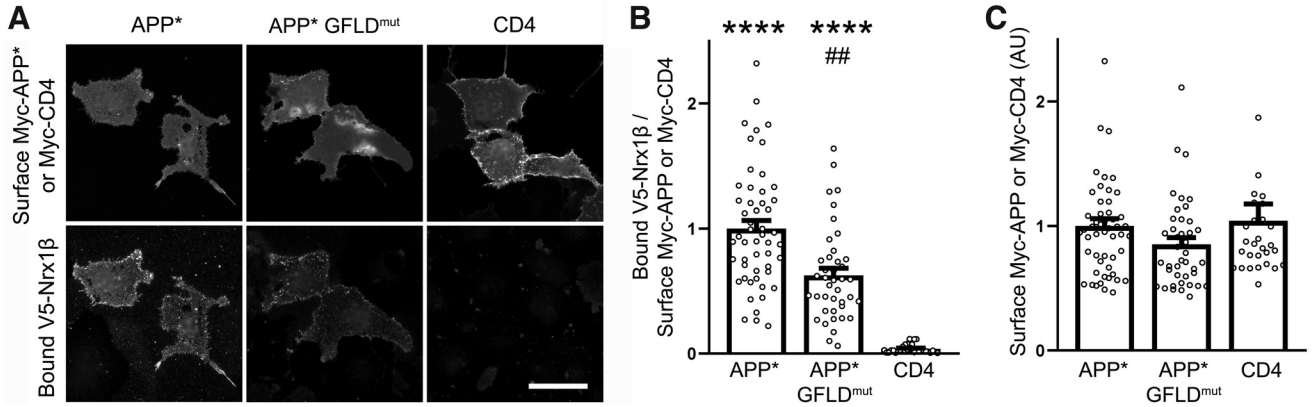

Figure 2. Full-length APP binds Nrx1β ectodomain, and binding is reduced for dimerization mutant GFLD^{mut}. ***A***, Myc tagged noncleavable APP*, APP* GFLD^{mut}, or CD4 control was expressed in COS-7 cells and incubated with purified soluble V5-Nrx1β ectodomain recombinant protein (100 nM). Cells were immunolabeled for cell surface Myc-APP or Myc-CD4 and bound V5-Nrx1β. ***B***, Binding of Nrx1β ectodomain to APP* and APP* GFLD^{mut} was significantly greater than binding to negative control CD4. $p < 0.0001$ (Kruskal–Wallis). $^{****}p < 0.0001$ compared with binding to CD4 (*post hoc* Dunn's multiple comparison tests). Compared with binding to APP*, Nrx1β ectodomain binding to APP* GFLD^{mut} was significantly reduced. $^{\#\#}p < 0.005$ compared with binding to APP* (Dunn's multiple comparison test). $n = 52$ cells for APP*, $n = 41$ for APP* GFLDmut, and $n = 31$ for CD4 from three independent experiments. ***C***, For all of the above binding assays, the COS-7 cells analyzed did not differ in surface expression of Myc tagged APP*, APP* GFLD^{mut}, or CD4. $p = 0.092$ (Kruskal–Wallis). Scale bars, 50 μm.

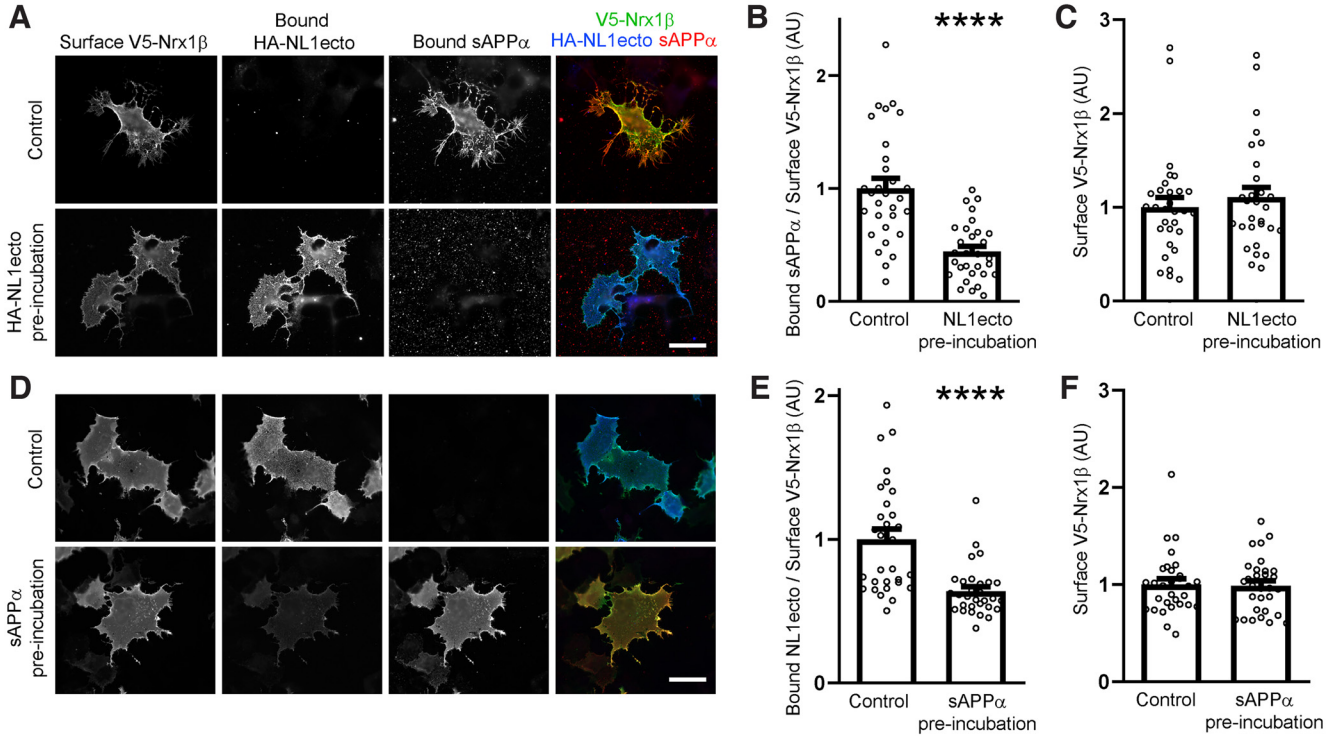

Figure 3. APP competes with NL for binding to β-Nrx. ***A***, COS-7 cells expressing V5-Nrx1β were pretreated with binding buffer alone (control) or containing soluble HA-NL1 ectodomain (HA-NL1ecto) before being incubated with sAPPα. Cells were immunolabeled for cell surface V5-Nrx1β, bound NBL1 ectodomain, and bound sAPPα. ***B***, NL1 ectodomain binding reduced the subsequent binding of sAPPα onto Nrx1β-expressing cells. $^{****}p < 0.0001$ (Mann–Whitney). $n = 30$ cells each from three independent experiments. ***C***, The COS-7 cells analyzed in ***B*** did not differ in surface expression of V5-Nrx1β. $p = 0.56$ (Mann–Whitney). ***D***, COS-7 cells expressing V5-Nrx1β were pretreated with binding buffer alone (control) or containing sAPPα before being incubated with soluble NL1 ectodomain. Cells were immunolabeled for cell surface V5-Nrx1β, bound NL1 ectodomain, and bound sAPPα. ***E***, sAPPα binding reduced the subsequent binding of NL1 ectodomain onto Nrx1β-expressing cells. $^{****}p < 0.0001$ (Mann–Whitney). $n = 30$ cells each from three independent experiments. ***F***, The COS-7 cells analyzed in ***E*** did not differ in surface expression of V5-Nrx1β. $p = 0.99$ (Mann–Whitney). Scale bars, 50 μm.

to Nrx1β, likely by binding to a common or overlapping surface of Nrx1β.

APP binding to Nrx-β is mediated by the LNS domain and modulated by splice site S4

The binding of NL1 to Nrx1β is calcium-dependent (Ichtchenko et al., 1995). We thus tested whether calcium is also required for APP binding to Nrx1β. Using a calcium-free binding buffer and the calcium chelator EDTA significantly reduced APP binding to Nrx1β (Fig. 4*A*,*B*). The binding of NL1 to Nrx1β is modulated by alternative splicing; affinity is reduced by inclusion of an insert at splice site 4 (S4) (Chih et al., 2006; Graf et al., 2006; Koehnke et al., 2010). Furthermore, other ligands LRRTMs only bind to Nrx

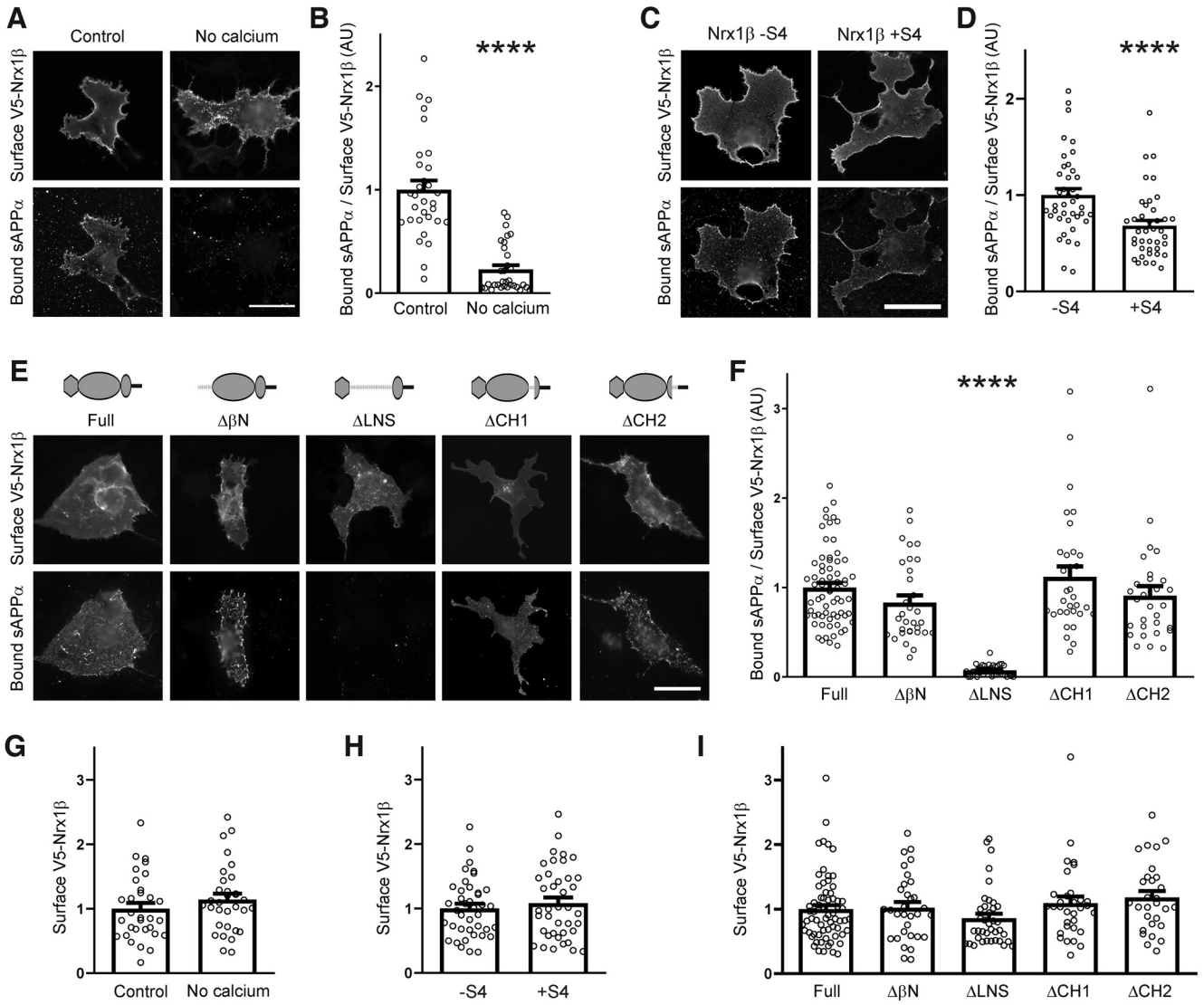

Figure 4. sAPPα binds the Nrx1β LNS domain in a calcium-dependent manner modulated by splice site S4. ***A***, Binding of sAPPα to V5-Nrx1β expressed on COS-7 cells is shown in normal binding buffer (control) or in binding buffer lacking calcium and containing 10 mM EGTA (no calcium). ***B***, Binding of sAPPα to V5-Nrx1β on COS-7 cells was calcium-dependent. ****$p < 0.0001$ (Mann–Whitney). $n = 31$ cells for control and $n = 32$ cells for the no calcium condition from three independent experiments. ***C***, Binding of sAPPα is shown to COS-7-cells expressing V5-Nrx1β lacking splice site 4 (–S4, used for all other experiments) or containing splice site 4 (+S4). ***D***, The presence of the Nrx1b splice site 4 insert reduced sAPPα binding. ****$p < 0.0001$ (Mann–Whitney). $n = 40$ cells each from three independent experiments. ***E***, Binding of sAPPα is shown to COS-7 cells expressing V5-tagged Nrx1β full-length or deletion mutants lacking the β-specific N-terminal region ($\Delta\beta$N), the LNS domain (ΔLNS), or each half of the glycosylated region (ΔCH1, ΔCH2). ***F***, The Nrx1β LNS domain mediates sAPPα binding on COS-7 cells. $p < 0.0001$ (Kruskal–Wallis). ****$p < 0.0001$ (Dunn's multiple comparison *post hoc* test), compared with Nrx1β full-length, $p > 0.999$ for the other construct comparisons with full-length. $n = 67$ cells for full-length, $n = 32$ for $\Delta\beta$N and ΔCH1, $n = 38$ for ΔLNS, and $n = 29$ for ΔCH2 from three independent experiments. ***G-I***, For all of the above binding assays, the COS-7 cells analyzed did not differ in surface expression of V5-Nrx. ***G***, $p = 0.283$ (Mann–Whitney) for calcium dependence. ***H***, $p = 0.656$ (Mann–Whitney) for effect of splice site 4. ***I***, $p = 0.058$ (Kruskal–Wallis) for the deletion mutants. Scale bars, 50 μm.

forms that lack an insert at S4, while cerebellins only bind to Nrx forms that contain an insert at S4 (Ko et al., 2009; Siddiqui et al., 2010; Uemura et al., 2010; Joo et al., 2011). We asked whether the presence of an insert at S4 regulates APP binding. We found a significant 32% decrease in the binding of APP to Nrx1β containing an insert at S4 compared with Nrx1β lacking an insert at S4 (Fig. 4*C*,*D*; all other experiments used Nrx forms lacking an S4 insert). Collectively, our data suggest that APP is a *bona fide* ligand of Nrx-β whose interaction is dependent on the presence of calcium and is modulated by alternative splicing. Furthermore, APP is most similar to NL1 (the major NL1 form containing the B insert) as being a specific ligand for Nrx-β and not Nrx-α and that binds Nrx-β forms lacking and containing the S4 insert with different affinity.

These findings suggest that APP might bind to the same region of Nrx-β as other major ligands, the LNS6 (Laminin Neurexin Sex hormone-binding protein) domain (Sudhof, 2017). To identify the domain of Nrx-β involved in APP binding, we tested binding of sAPPα to a series of deletion mutants of Nrx1β expressed on COS-7 cells. Deleting the LNS domain of Nrx1β effectively abolished APP binding, while deleting any other domain had no effect (Fig. 4*E*,*F*). Thus, the Nrx-β domain for binding of APP, the LNS domain, is the same as that for other synaptogenic ligands NLs, LRRTMs, and cerebellins (Sudhof, 2017). Importantly, this high-affinity binding site for APP in the LNS domain is distinct from lower-affinity binding site for Aβ in the β-specific N-terminal region (Naito et al., 2017).

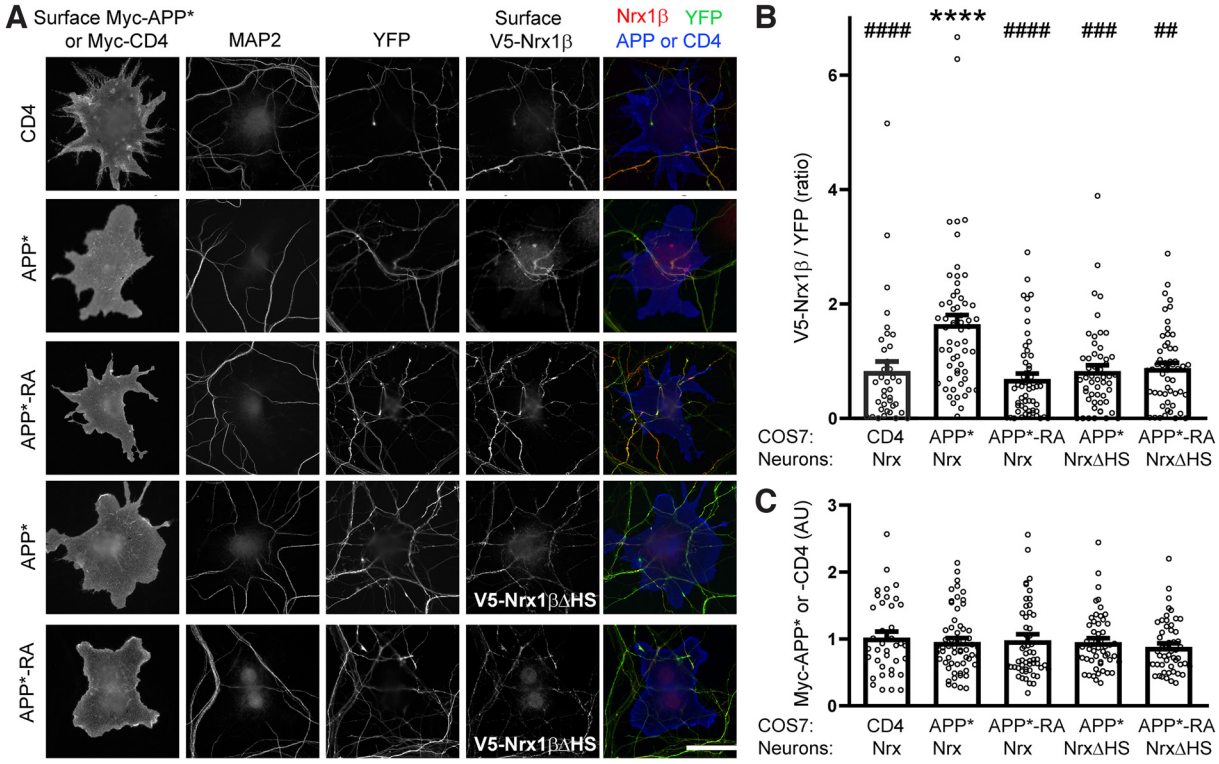

Figure 5. APP recruitment of neuronal Nrx1β requires APP HS binding sites and Nrx HS modification. ***A***, Hippocampal neurons were transfected at plating with the construct YFP-P2A-V5-Nrx1β or the mutant lacking HS modification YFP-P2A-V5-Nrx1β ΔHS. The P2A peptide linker mediates coexpression of YFP and the V5-tagged Nrx. COS-7 cells were transfected to expressed Myc-tagged APP* (APPΔ592-621 to reduce ectodomain cleavage to maximize surface expression), APP*-RA with mutations in HS binding sites (KRGR-AAAA in E1 and HRER-AAAA in E2), or CD4-negative control, and cocultured with the transfected neurons. Cocultures were immunolabeled for surface V5, surface Myc, and the dendrite marker MAP2 and assessed for recruitment of the V5-Nrx on YFP-positive axons at sites of contact with Myc-positive COS-7 cells. ***B***, ***C***, Nrx1β but not Nrx1β ΔHS was recruited to contact sites with COS-7 cells expressing Myc-APP* but not Myc-APP*-RA. Recruitment was assessed as the ratio of surface V5-Nrx to YFP at YFP-positive axon contact sites with COS-7 cells positive for surface expression of the Myc-tagged CD4, APP*, or APP*-RA. $p < 0.0001$ (Kruskal–Wallis). $^{****}p < 0.0001$ (Dunn's multiple comparison *post hoc* test), compared with CD4 Nrx. $p > 0.999$ for the other comparisons with CD4 Nrx. $^{\#\#}p = 0.002$, $^{\#\#\#}p = 0.0002$, and $^{\#\#\#\#}p < 0.0001$ compared with APP* Nrx (all Dunn's multiple comparison *post hoc* tests). $n = 37$ cells for CD4 Nrx, $n = 59$ for APP* Nrx, $n = 54$ for APP*-RA Nrx, $n = 52$ for APP* NrxΔHS, and $n = 53$ for APP*-RA NrxΔHS from three independent experiments (***B***). COS-7 cells with equal cell surface expression were selected for analysis. $p = 0.730$ (Kruskal–Wallis) (***C***). Scale bars, 50 μm.

APP recruits axonal Nrx-β in an HS-dependent manner

To assess the APP-Nrx interaction in a somewhat more physiological context, we used a cell-based recruitment assay similar to that performed previously for NL1 and LRRTM2. These Nrx ligands expressed on COS-7 cells cocultured with neurons are able to recruit recombinant axonal Nrx to contact sites (Zhang et al., 2018). Thus, we tested whether the surface-expressed APP* on COS-7 cells is able to recruit Nrx at axon contact sites. To normalize for differences in expression level per neuron and in COS-7 cell contact area for the recombinant Nrx1β in axons, we expressed V5-Nrx1β in neurons in an equimolar ratio with YFP using the self-cleaving peptide P2A (Kim et al., 2011). Our measure of recruitment was the total intensity of surface V5-Nrx divided by the total intensity of YFP at contact areas of transfected axons with transfected COS-7 cells. We found that axonal surface V5-Nrx1β was significantly recruited to contact sites with COS-7 cells expressing the noncleavable Myc-APP* to a higher level than with COS-7 cells expressing an unrelated control protein Myc-CD4 (Fig. 5). This finding indicates the formation of a complex involving full-length APP in *trans* with axonal Nrx1β, supporting the possibility that axonal Nrx might mediate the synaptogenic activity of APP.

It was recently shown that HS modification of Nrx provides a second site for NL binding along with the LNS domain, and this HS modification of Nrx1 is essential for proper synapse development and mouse survival (Zhang et al., 2018). The HS modification occurs in the region deleted in the Nrx1β ΔCH2 construct assayed in Figure 4*E*, *F*. However, Nrx overexpressed in cell lines is mostly lacking the HS modification (Zhang et al., 2018), so any potential role for Nrx HS modification in interaction with APP may have been missed in these assays in non-neuronal cells. Since APP is a well-known HS-binding protein (Smith et al., 2015; Muller et al., 2017), it seems likely that the HS chain on neuronal Nrx may be a second binding site for APP along with the Nrx LNS protein domain binding site identified in Figure 4*E*, *F*.

To test the role of HS in the formation of the trans-cellular complex involving APP and neuronal Nrx1β, we performed the cell-based recruitment assay with APP*-RA with mutations in HS-binding sites or Nrx1β ΔHS lacking HS modification. APP*-RA has mutations in key residues of the high-affinity HS-binding sites of APP in the E1 domain (amino acids 99-102 KRGR-AAAA) (Small et al., 1994) and in the E2 domain (amino acids 327-330 HRER-AAAA) (Multhaup, 1994; Multhaup et al., 1995). Nrx1β ΔHS bears a single amino acid mutation of the Ser that is normally HS modified to Ala thus blocking HS modification (LVASAEC to LVAAAEC) (Zhang et al., 2018). These mutants APP*-RA and Nrx1β ΔHS traffic well to the cell surface (Fig. 5) and do not affect APP-Nrx binding via protein domains in non-neuronal cells (data not shown), supporting the specificity of the mutations for disrupting the HS-mediated interaction site between APP and neuronal Nrx. In contrast to the recruitment

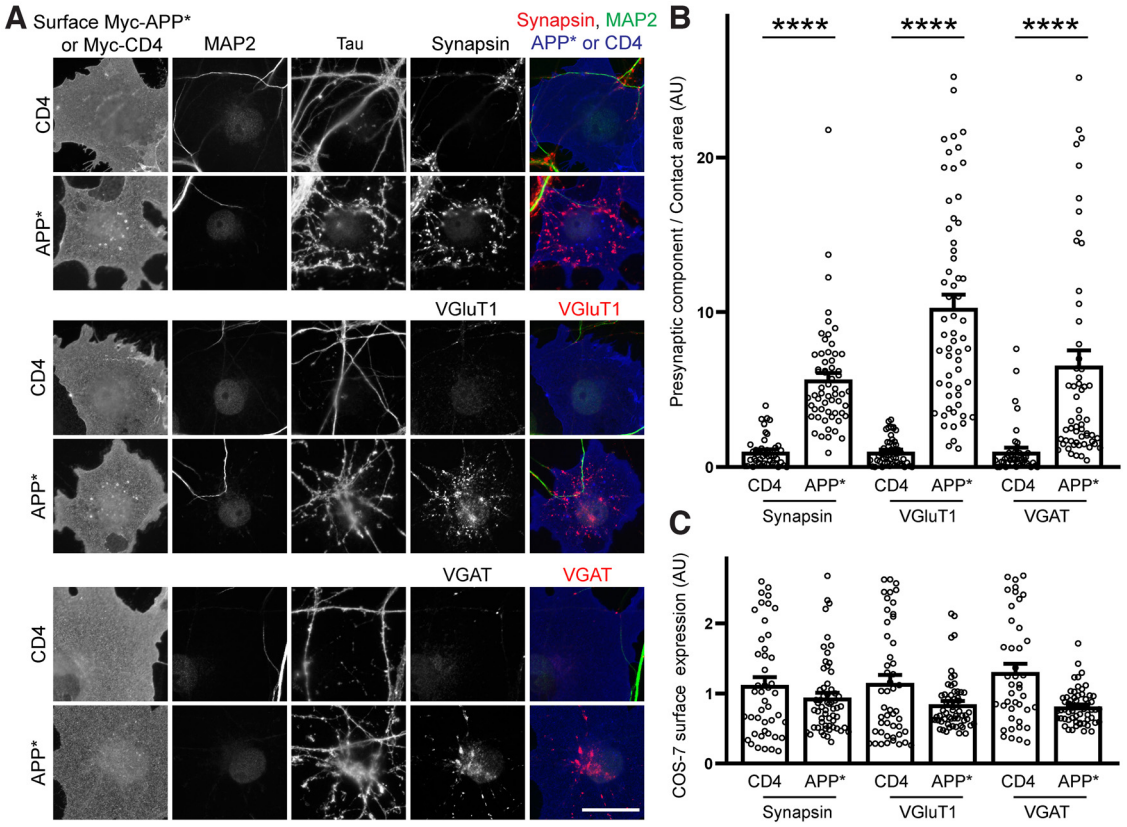

Figure 6. APP induces glutamatergic and GABAergic presynaptic differentiation in coculture. ***A***, Myc-APP* or negative control Myc-CD4 were expressed in COS-7 cells, which were cocultured with hippocampal neurons. APP* but not CD4 on COS-7 cells induced clustering of synapsin, VGluT1, and VGAT along contacting tau-positive axons. Induced clusters were distinguished from native synapses by lack of contact with MAP2-positive dendrites. ***B***, APP* induced significant clustering of synapsin, VGluT1, and VGAT relative to CD4, measured as the total intensity of punctate presynaptic component per contact area of tau-positive axons with expressing COS-7 cells, excluding contact areas with MAP2-positive dendrites. $p < 0.0001$ (Kruskal–Wallis). ****$p < 0.0001$ (Dunn's multiple comparison *post hoc* test), comparing APP* with CD4 for each presynaptic component. $n = 59$ cells for APP* groups, $n = 45$ for CD4 synapsin, $n = 49$ for CD4 VGluT1, and $n = 42$ for CD4 VGAT from three independent experiments. ***C***, COS-7 cells with equal cell surface expression were selected for analysis. $p = 0.071$ (Kruskal–Wallis). Scale bars, 50 μm.

by APP* of Nrx1β, APP*-RA was unable to recruit neuronal Nrx1β and APP* was unable to recruit neuronal Nrx1$\beta\Delta$HS above the background level of the negative control (Fig. 5). Thus, both high-affinity HS binding by APP and HS modification of Nrx1β are required for formation of the APP Nrx complex in this recruitment assay. These results are similar to results found previously for NL1 and LRRTM2, where interactions between these ligands and the Nrx LNS protein domain were sufficient to mediate binding of purified ectodomain proteins but not sufficient to mediate trans-cellular recruitment on axons (Zhang et al., 2018). For axonal recruitment, the additional interaction between NL1 or LRRTM2 and the Nrx HS chain was required. Similarly, our data together show that APP binds to the Nrx LNS protein domain but that additional interaction of APP with the Nrx HS chain is needed for trans-cellular recruitment on axons. The difference in requirements among the binding and recruitment assays may reflect a simple need for higher-affinity interaction for trans-cellular recruitment or a more complex role of the HS-mediated interaction in stabilizing axon surface complexes.

APP induces glutamatergic and GABAergic presynaptic differentiation in coculture

Coculture of non-neuronal cells expressing APP or APP* with neurons has previously been shown to trigger presynaptic differentiation in contacting axons, assessed by local clustering of synaptophysin (Wang et al., 2009; Stahl et al., 2014). We confirmed the ability of APP* in COS-7 cells to trigger presynaptic differentiation in contacting hippocampal axons, assessed by local clustering of synapsin (Fig. 6), a component present at all presynaptic sites similar to synaptophysin. Synaptogenic factors can differ in their ability to trigger glutamatergic or GABAergic presynaptic differentiation, assessed by local clustering of VGluT1 or of VGAT in contacting axons, presumably reflecting selective expression of binding partners on the axons. Selectivity in coculture typically reflects a selective *in vivo* function. For example, Slitrk3 induces clustering of VGAT but not VGluT1 in coculture and *Slitrk3*$^{-/-}$ mice show deficits in GABAergic but not glutamatergic synaptic density and function (Takahashi et al., 2012). We found that APP* induces robust clustering of both VGluT1 and VGAT in coculture (Fig. 6). These findings are consistent with the expression of the APP binding partner Nrx-β in both glutamatergic and GABAergic axons and suggest that the APP-Nrx-β complex may function at both synapse types.

The synaptogenic activity of APP requires HS binding and axonal Nrx

We next tested whether HS binding by APP is required for its synaptogenic activity, its ability to induce presynaptic differentiation in a coculture hemi-synapse formation assay. In contrast to the ability of APP* on COS-7 cells to trigger synapsin clustering in contacting axons, mutation of the high-affinity HS binding sites in APP*-RA completely abolished synaptogenic activity to a

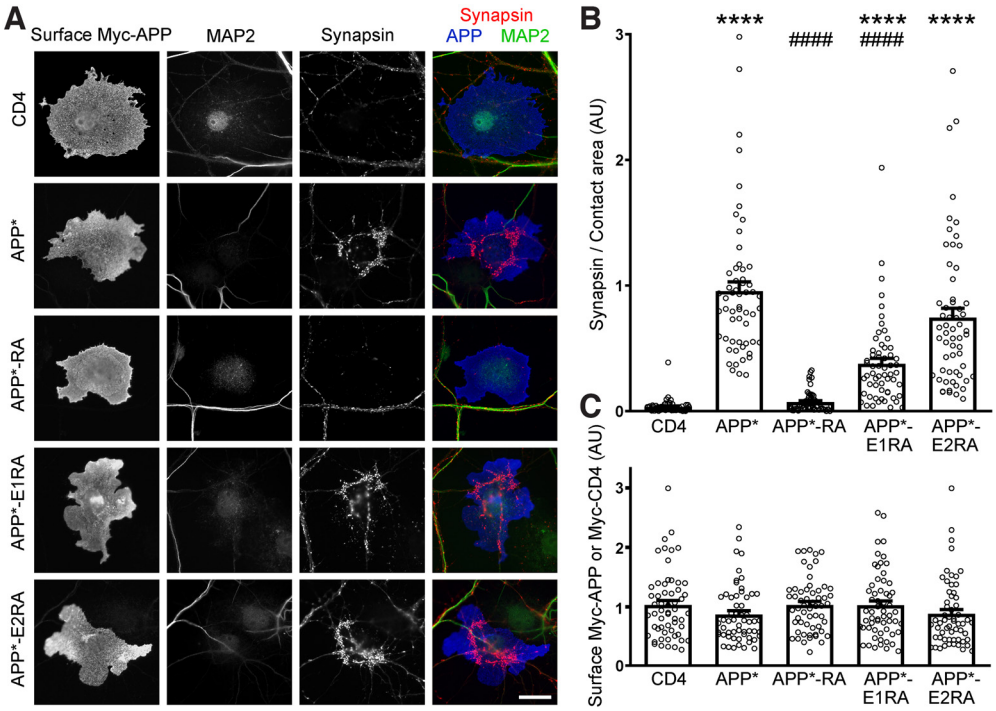

Figure 7. Presynaptic differentiation induced by APP in coculture requires both E1 and E2 domain APP high-affinity HS binding sites. ***A***, Myc-tagged APP*, APP*-E1RA with mutation KRGR-AAAA in the E1 domain high-affinity HS binding site, APP*-E2RA with mutation HRER-AAAA in the E2 domain high-affinity HS binding site, APP*-RA with both KRGR-AAAA E1 domain and HRER-AAAA E2 domain mutations or negative control CD4 were expressed in COS-7 cells, which were cocultured with hippocampal neurons. APP*, APP*-E1RA, and APP*-E2RA but not APP*-RA or CD4 on COS-7 cells induced clustering of synapsin along contacting axons. Induced clusters of synapsin were distinguished from native synapses by lack of contact with MAP2-positive dendrites. ***B***, ***C***, Mutation of both E1 and E2 domain high-affinity HS binding sites, but not of either alone, abolished presynaptic differentiation induced by APP*. Presynaptic differentiation was assessed as the total intensity of punctate synapsin per contact area of axons with expressing COS-7 cells, excluding contact areas with MAP2-positive dendrites. $p < 0.0001$ (Kruskal–Wallis). ****$p < 0.0001$ (Dunn's multiple comparison *post hoc* test), compared with negative control CD4. $p > 0.999$ for APP*-RA compared with CD4. $^{\#\#\#\#}p < 0.0001$ compared with APP*. $p = 0.785$ for APP*-E2RA compared with APP* (all Dunn's multiple comparison *post hoc* tests). $n = 57$ cells for APP*, APP*-E1RA, and CD4, and $n = 58$ for APP*-RA and APP*-E2RA from three independent experiments (***B***). COS-7 cells with equal cell surface expression were selected for analysis. $p = 0.076$ (Kruskal–Wallis) (***C***). Scale bars, 30 μm.

level indistinguishable from the negative control protein CD4 (Fig. 7). We also assessed mutations in either the E1 or E2 domains separately. The APP*-E2RA mutation alone had no effect, while the APP*-E1RA mutation reduced synaptogenic activity compared with APP* but still retained synaptogenic activity compared with negative control CD4 (Fig. 7). These data suggest that the synaptogenic activity of APP requires an HS-dependent interaction to which the E1 and E2 domains both contribute.

Nrxs are prime candidates to mediate the synaptogenic activity of APP via HS (Fig. 5) and LNS domain (Fig. 3) interactions. To directly test the role of Nrxs, we reduced the expression of all three Nrx genes by 85% in primary hippocampal cultures by using AAV-mediated triple knockdown (AAV-shNrx modified from Zhang et al., 2018) (Fig. 8*A*,*B*). We then cocultured these neurons with COS-7 cells that were transfected with NL2 as a control that functions through Nrx, NGL-3 as a control that functions through PTPs independently of Nrx (Bomkamp et al., 2019; Roppongi et al., 2020), or APP*. As expected, Nrx knockdown reduced the ability of NL2 but had no effect on the ability of NGL-3 to induce presynaptic differentiation in hippocampal cultures (Fig. 8*C*–*E*). Confirming our hypothesis, we found that Nrx knockdown significantly reduced the ability of APP* to induce presynaptic differentiation (Fig. 8*C*–*E*). Thus, Nrx mediates the synaptogenic activity of APP.

Discussion

In this study, we identify the presynaptic hub Nrx as a binding partner of APP and mediator of the synaptogenic activity of APP. We find that APP shares similarities with other synaptogenic partners of Nrx, NLs, and LRRTM 1 and 2, in exhibiting a dual binding mode: calcium-dependent binding to the Nrx LNS6 protein domain and binding to the HS glycan chain. Similar to NL1 (the major NL1 form containing the B insert), APP is a specific ligand for Nrx-β but not Nrx-α and the S4 insert reduces but does not abolish binding. Furthermore, NL1 and APP compete for binding to Nrx-β, confirming an overlap in their binding interfaces. Axonal Nrx is recruited by APP *in trans*, dependent on the HS modification of Nrx and HS binding sites in APP. Moreover, as shown by Nrx triple knockdown, axonal Nrx is essential for presynaptic differentiation triggered by APP. Together, these findings deepen our understanding of the physiological roles of full-length APP at the synapse. Furthermore, the high-affinity interaction of Nrx observed with sAPPβ and sAPPα as well as full-length APP raise new directions for investigation into mechanisms underlying early synaptic deficits in AD.

Based on the domain mapping, regulation by S4, and competition with NL1, APP is yet another Nrx ligand that binds the same face of LNS6 as do NLs, LRRTM 1 and 2, and cerebellins (Sudhof, 2017; Gomez et al., 2021). Regulation of Nrx S4 splicing occurs in a cell type-specific manner, during development, and by pharmacological or behaviorally induced changes in neuronal activity (Gomez et al., 2021), thus providing a wide range of situations for S4 modulation of the APP-Nrx interaction. Also like NLs and LRRTM 1 and 2 (Zhang et al., 2018), APP binds HS (Multhaup, 1994; Smith et al., 2015). HS modification of Nrx is required for recruitment of axonal Nrx by APP in coculture, indicating that the APP-LNS interaction is not sufficient. The

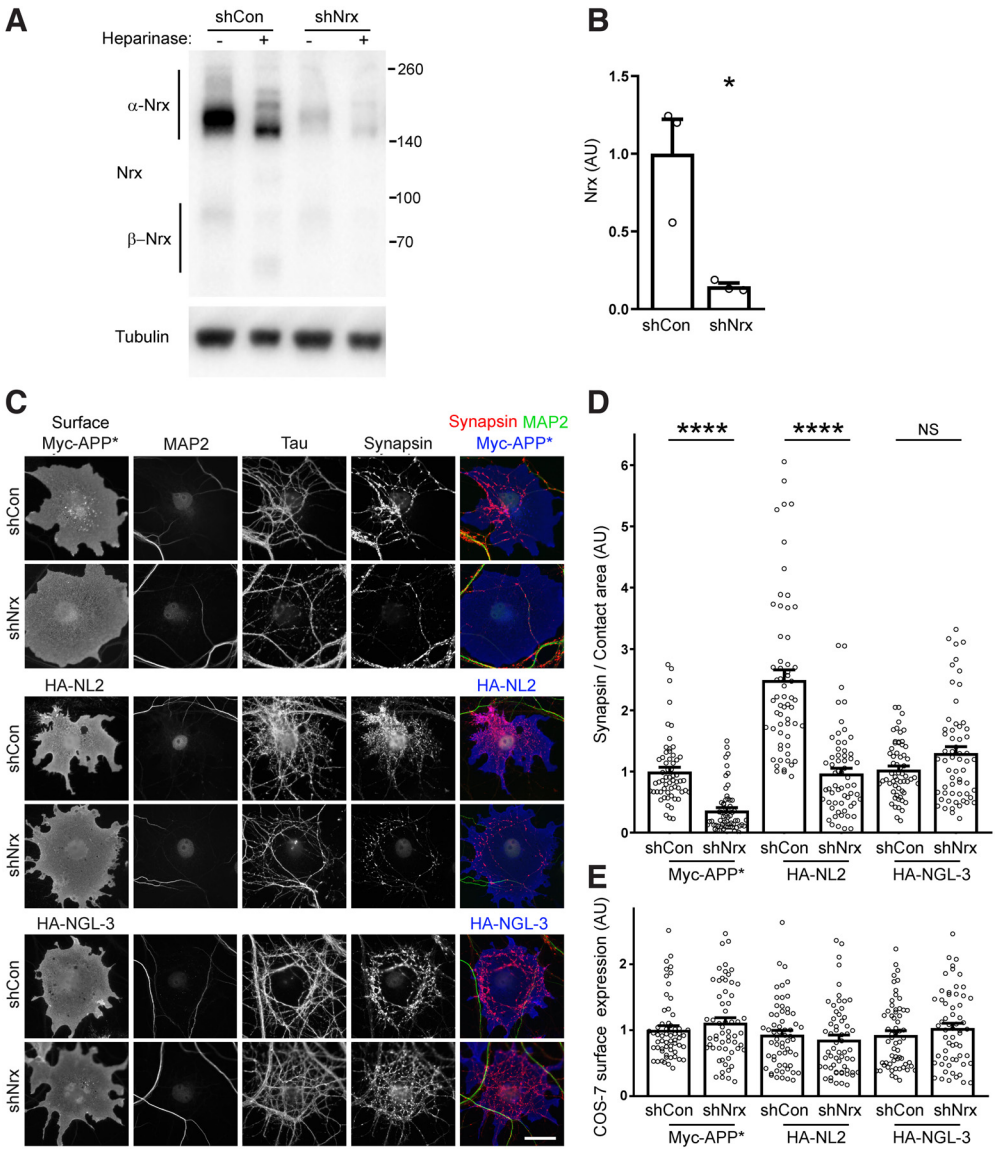

Figure 8. Presynaptic differentiation induced by APP in coculture requires axonal Nrx. ***A***, ***B***, Hippocampal neurons were transduced with an AAV vector expressing control shRNAs (shCon) or expressing shRNAs for triple knockdown of Nrx 1, 2, and 3 (shNrx). Lysate was immunoblotted for Nrx, which shows the expected reduction in molecular weight on heparinase treatment to remove the HS modification. Relative to shCon, shNrx treatment resulted in an 85% reduction in Nrx protein measuring the main α-Nrx band normalized to tubulin. *$p = 0.0186$ (*t* test). $n = 3$ cultures. ***C***, Hippocampal neurons were transduced with AAV expressing shNrx or shCon and then cocultured with COS-7 cells. COS-7 cells expressing Myc-APP*, HA-NL2, or HA-NGL-3 induced clusters of synapsin on contacting axons at regions lacking MAP2-positive dendrite contact. Synapsin clustering induced by APP* and by the Nrx ligand NL2 was markedly reduced by Nrx triple knockdown, whereas there was no obvious effect on synapsin clustering induced by the PTP ligand NGL-3. ***D***, ***E***, Presynaptic differentiation by APP* was reduced by triple knockdown of Nrx. Presynaptic differentiation was assessed as the total intensity of punctate synapsin per contact area of axons with expressing COS-7 cells, excluding contact areas with MAP2-positive dendrites. $p < 0.0001$ (Kruskal–Wallis). ****$p < 0.0001$ or NS, Not significant $p > 0.999$, comparing each shNrx with shCon (Dunn's multiple comparison *post hoc* tests). $n = 59$ cells for APP* shCon and APP* shNrx and $n = 60$ cells for all other groups, from three independent experiments (***B***). COS-7 cells with equal cell surface expression were selected for analysis. $p = 0.494$ (Kruskal–Wallis) (***C***). Scale bars, 50 μm.

dual binding mode of APP to Nrx LNS6 and HS glycan, with HS binding not just modulatory but essential for APP synaptogenic function, is further supported by the inability of APP-RA with mutations in HS binding sites to recruit axonal Nrx or to induce presynaptic differentiation.

Our data are consistent with two possible models through which dendritic APP and axonal Nrx promote presynaptic differentiation. The simplest model is that dendritic APP binds axonal Nrx *in trans* to trigger presynaptic differentiation, similar to the actions of NLs and LRRTMs. An alternate model is that dendritic APP binds axonal APP, which together bind axonal Nrx (i.e., an APP *trans* dimer binds Nrx to trigger presynaptic differentiation). This alternate model is favored considering our work together with the findings that axonal APP and APP dimerization are needed for presynaptic differentiation induced by APP in coculture (Wang et al., 2009; Baumkotter et al., 2014). An APP *trans* dimer might be needed to stabilize full-length APP on the surface and/or to present an optimum conformation for Nrx binding. Our data support a role of APP dimerization in Nrx binding, although in an assay promoting *cis* rather than *trans* APP dimerization. Regardless of the form of the APP-Nrx transsynaptic complex, the resultant local clustering of Nrx on the axon surface is likely essential and may be sufficient to trigger presynaptic differentiation (Dean et al., 2003), although axonal signaling through the intracellular domain of APP may also be involved (Wang et al., 2009). Importantly, Nrx is acting as a

mediator and not as a generic permissive factor, as Nrx is not required for presynaptic differentiation induced by the PTP ligand NGL-3 but only for presynaptic differentiation induced by Nrx ligands including APP. This form of synaptic organizing complex with Nrx binding to a *trans* dimer of a presynaptic and postsynaptic transmembrane protein (APP-APP) would be distinct from the classic forms of Nrx binding to a postsynaptic transmembrane protein (NL or LRRTM) or to a soluble protein, which in turn binds a postsynaptic transmembrane protein (cerebellin-GluD).

These trans-synaptic complexes of Nrx and postsynaptic ligands promote synapse development as cell adhesion molecules, stabilizing the axon-dendrite contacts and recruiting additional components through molecular interactions on both sides of the synapse (Sudhof, 2017; Gomez et al., 2021). Simply binding to Nrx is not sufficient to promote synaptic differentiation. For example, the soluble Nrx ligand cerebellin promotes synapse development only by simultaneously binding to the postsynaptic transmembrane protein GluD to form a trans-synaptic adhesion complex (Yuzaki and Aricescu, 2017). Conversely, ectodomain cleavage of postsynaptic Nrx ligand NL1 destabilizes presynaptic Nrx and reduces transmitter release (Peixoto et al., 2012). Cleavage of full-length APP also reduces its synapse-promoting activity. Stahl et al. (2014) showed that deleting the α and β secretase cleavage sites to generate a noncleavable APP (the APP* used here) increases its synaptogenic activity in coculture. Thus, our model is that binding of full-length APP to Nrx is synapse promoting, linking the postsynaptic and presynaptic membranes. sAPPα and sAPPβ also bind Nrx with high affinity yet lack any link to the postsynaptic membrane. Furthermore, sAPP and NL1 compete for binding to Nrx. Thus, we suggest that sAPPα and sAPPβ may interfere with the synapse-promoting functions of Nrx by blocking Nrx from binding to a subset of transmembrane synaptogenic ligands, including full-length APP and NL1.

The *in vivo* functions of the APP-Nrx-β interaction may be complex, regulated by local levels of APP cleavage with potential competition from soluble sAPP-Nrx-β limiting the synapse-promoting functions of full-length APP-Nrx-β and of NL1-Nrx-β. Our data also suggest that APP-Nrx-β complexes may function at both glutamatergic and GABAergic synapses. $APP^{-/-}$ mice show some age-dependent changes at glutamatergic and GABAergic synapses, in spine density and in forms of synaptic plasticity (for review, see Muller et al., 2017). Conditional KO of Nrx-β in excitatory postnatal neurons suppresses transmitter release and alters plasticity in a subset of circuits (Anderson et al., 2015). *In vivo* mutation of other Nrx ligands NLs and LRRTMs that are synaptogenic in the coculture assay can affect a range of synaptic properties, including synapse density, morphology, transmitter release probability, receptor composition, and long-term plasticity (Roppongi et al., 2017; Sudhof, 2017; Gomez et al., 2021). Further work will be needed to develop tools to specifically perturb the APP-Nrx-β interaction to define its role in synapse development and plasticity in brain circuits.

These findings may have implications for AD, providing novel mechanisms that may contribute to the early synaptic deficits. Altered cleavage of APP associated with mutations in APP may change the balance of multiple APP products, full-length APP and/or sAPPs, as well as Aβ. Any change in the level of full-length APP-Nrx, sAPPα-Nrx, or sAPPβ-Nrx complexes could have consequences for synaptic function. The Nrx synaptogenic complexes are important not just in development but also at mature synapses; for example, deletion of NL1 after synapse formation perturbs NMDAR currents and synaptic plasticity (Jiang et al., 2017). Beyond its role in dementia, the APP gene is triplicated in Down syndrome, and overexpression of WT human APP in mice leads to synaptic deficits without plaques (Mucke et al., 2000). By increasing our knowledge of the molecular interactions of APP and its roles in the fundamental process of synaptic differentiation, we may better understand how alterations in APP impact synaptic function in neurologic diseases.

References

Alvarez VA, Ridenour DA, Sabatini BL (2006) Retraction of synapses and dendritic spines induced by off-target effects of RNA interference. J Neurosci 26:7820–7825.

Anderson GR, Aoto J, Tabuchi K, Foldy C, Covy J, Yee AX, Wu D, Lee SJ, Chen L, Malenka RC, Sudhof TC (2015) β-Neurexins control neural circuits by regulating synaptic endocannabinoid signaling. Cell 162:593–606.

Aoto J, Foldy C, Ilcus SM, Tabuchi K, Sudhof TC (2015) Distinct circuit-dependent functions of presynaptic neurexin-3 at GABAergic and glutamatergic synapses. Nat Neurosci 18:997–1007.

Aricescu AR, Lu W, Jones EY (2006) A time- and cost-efficient system for high-level protein production in mammalian cells. Acta Crystallogr D Biol Crystallogr 62:1243–1250.

Baumkotter F, Schmidt N, Vargas C, Schilling S, Weber R, Wagner K, Fiedler S, Klug W, Radzimanowski J, Nickolaus S, Keller S, Eggert S, Wild K, Kins S (2014) Amyloid precursor protein dimerization and synaptogenic function depend on copper binding to the growth factor-like domain. J Neurosci 34:11159–11172.

Bomkamp C, Padmanabhan N, Karimi B, Ge Y, Chao JT, Loewen CJ, Siddiqui TJ, Craig AM (2019) Mechanisms of PTPσ-mediated presynaptic differentiation. Front Synaptic Neurosci 11:17.

Boucard AA, Chubykin AA, Comoletti D, Taylor P, Sudhof TC (2005) A splice code for trans-synaptic cell adhesion mediated by binding of neuroligin 1 to alpha- and beta-neurexins. Neuron 48:229–236.

Canter RG, Penney J, Tsai LH (2016) The road to restoring neural circuits for the treatment of Alzheimer's disease. Nature 539:187–196.

Chih B, Gollan L, Scheiffele P (2006) Alternative splicing controls selective trans-synaptic interactions of the neuroligin-neurexin complex. Neuron 51:171–178.

de Wilde MC, Overk CR, Sijben JW, Masliah E (2016) Meta-analysis of synaptic pathology in Alzheimer's disease reveals selective molecular vesicular machinery vulnerability. Alzheimers Dement 12:633–644.

Dean C, Scholl FG, Choih J, DeMaria S, Berger J, Isacoff E, Scheiffele P (2003) Neurexin mediates the assembly of presynaptic terminals. Nat Neurosci 6:708–716.

Gomez AM, Traunmuller L, Scheiffele P (2021) Neurexins: molecular codes for shaping neuronal synapses. Nat Rev Neurosci 22:137–151.

Graf ER, Zhang X, Jin SX, Linhoff MW, Craig AM (2004) Neurexins induce differentiation of GABA and glutamate postsynaptic specializations via neuroligins. Cell 119:1013–1026.

Graf ER, Kang Y, Hauner AM, Craig AM (2006) Structure function and splice site analysis of the synaptogenic activity of the neurexin-1 β LNS domain. J Neurosci 26:4256–4265.

Ichtchenko K, Hata Y, Nguyen T, Ullrich B, Missler M, Moomaw C, Sudhof TC (1995) Neuroligin 1: a splice site-specific ligand for β-neurexins. Cell 81:435–443.

Jeong J, Paskus JD, Roche KW (2017) Posttranslational modifications of neuroligins regulate neuronal and glial signaling. Curr Opin Neurobiol 45:130–138.

Jiang M, Polepalli J, Chen LY, Zhang B, Sudhof TC, Malenka RC (2017) Conditional ablation of neuroligin-1 in CA1 pyramidal neurons blocks LTP by a cell-autonomous NMDA receptor-independent mechanism. Mol Psychiatry 22:375–383.

Joo JY, Lee SJ, Uemura T, Yoshida T, Yasumura M, Watanabe M, Mishina M (2011) Differential interactions of cerebellin precursor protein (Cbln) subtypes and neurexin variants for synapse formation of cortical neurons. Biochem Biophys Res Commun 406:627–632.

Kaech S, Banker G (2006) Culturing hippocampal neurons. Nat Protoc 1:2406–2415.

Kim JH, Lee SR, Li LH, Park HJ, Park JH, Lee KY, Kim MK, Shin BA, Choi SY (2011) High cleavage efficiency of a 2A peptide derived from porcine teschovirus-1 in human cell lines, zebrafish and mice. PLoS One 6: e18556.

Ko J, Fuccillo MV, Malenka RC, Sudhof TC (2009) LRRTM2 functions as a neurexin ligand in promoting excitatory synapse formation. Neuron 64:791–798.

Koehnke J, Katsamba PS, Ahlsen G, Bahna F, Vendome J, Honig B, Shapiro L, Jin X (2010) Splice form dependence of β-neurexin/neuroligin binding interactions. Neuron 67:61–74.

Kohli BM, Pflieger D, Mueller LN, Carbonetti G, Aebersold R, Nitsch RM, Konietzko U (2012) Interactome of the amyloid precursor protein APP in brain reveals a protein network involved in synaptic vesicle turnover and a close association with Synaptotagmin-1. J Proteome Res 11:4075–4090.

Missler M, Zhang W, Rohlmann A, Kattenstroth G, Hammer RE, Gottmann K, Sudhof TC (2003) Alpha-neurexins couple Ca^{2+} channels to synaptic vesicle exocytosis. Nature 423:939–948.

Mucke L, Masliah E, Yu GQ, Mallory M, Rockenstein EM, Tatsuno G, Hu K, Kholodenko D, Johnson-Wood K, McConlogue L (2000) High-level neuronal expression of abeta 1-42 in wild-type human amyloid protein precursor transgenic mice: synaptotoxicity without plaque formation. J Neurosci 20:4050–4058.

Muller UC, Deller T, Korte M (2017) Not just amyloid: physiological functions of the amyloid precursor protein family. Nat Rev Neurosci 18:281–298.

Multhaup G (1994) Identification and regulation of the high affinity binding site of the Alzheimer's disease amyloid protein precursor (APP) to glycosaminoglycans. Biochimie 76:304–311.

Multhaup G, Mechler H, Masters CL (1995) Characterization of the high affinity heparin binding site of the Alzheimer's disease beta A4 amyloid precursor protein (APP) and its enhancement by zinc(II). J Mol Recognit 8:247–257.

Naito Y, Tanabe Y, Lee AK, Hamel E, Takahashi H (2017) Amyloid-beta oligomers interact with neurexin and diminish neurexin-mediated excitatory presynaptic organization. Sci Rep 7:42548.

Niemi JP, DeFrancesco-Lisowitz A, Cregg JM, Howarth M, Zigmond RE (2016) Overexpression of the monocyte chemokine CCL2 in dorsal root ganglion neurons causes a conditioning-like increase in neurite outgrowth and does so via a STAT3 dependent mechanism. Exp Neurol 275:25–37.

Peixoto RT, Kunz PA, Kwon H, Mabb AM, Sabatini BL, Philpot BD, Ehlers MD (2012) Transsynaptic signaling by activity-dependent cleavage of neuroligin-1. Neuron 76:396–409.

Pettem KL, Yokomaku D, Takahashi H, Ge Y, Craig AM (2013) Interaction between autism-linked MDGAs and neuroligins suppresses inhibitory synapse development. J Cell Biol 200:321–336.

Reissner C, Runkel F, Missler M (2013) Neurexins. Genome Biol 14:213.

Rice HC, de Malmazet D, Schreurs A, Frere S, Van Molle I, Volkov AN, Creemers E, Vertkin I, Nys J, Ranaivoson FM, Comoletti D, Savas JN, Remaut H, Balschun D, Wierda KD, Slutsky I, Farrow K, De Strooper B, de Wit J (2019) Secreted amyloid-beta precursor protein functions as a GABABR1a ligand to modulate synaptic transmission. Science 363: eaao4827.

Rolland M, Powell R, Jacquier-Sarlin M, Boisseau S, Reynaud-Dulaurier R, Martinez-Hernandez J, Andre L, Borel E, Buisson A, Lante F (2020) Effect of Abeta oligomers on neuronal APP triggers a vicious cycle leading to the propagation of synaptic plasticity alterations to healthy neurons. J Neurosci 40:5161–5176.

Roppongi RT, Karimi B, Siddiqui TJ (2017) Role of LRRTMs in synapse development and plasticity. Neurosci Res 116:18–28.

Roppongi RT, Dhume SH, Padmanabhan N, Silwal P, Zahra N, Karimi B, Bomkamp C, Patil CS, Champagne-Jorgensen K, Twilley RE, Zhang P, Jackson MF, Siddiqui TJ (2020) LRRTMs organize synapses through differential engagement of neurexin and PTPσ. Neuron 106:701.

Scheiffele P, Fan J, Choih J, Fetter R, Serafini T (2000) Neuroligin expressed in nonneuronal cells triggers presynaptic development in contacting axons. Cell 101:657–669.

Schilling S, Mehr A, Ludewig S, Stephan J, Zimmermann M, August A, Strecker P, Korte M, Koo EH, Muller UC, Kins S, Eggert S (2017) APLP1 is a synaptic cell adhesion molecule, supporting maintenance of dendritic spines and basal synaptic transmission. J Neurosci 37:5345–5365.

Selkoe DJ, Hardy J (2016) The amyloid hypothesis of Alzheimer's disease at 25 years. EMBO Mol Med 8:595–608.

Siddiqui TJ, Pancaroglu R, Kang Y, Rooyakkers A, Craig AM (2010) LRRTMs and neuroligins bind neurexins with a differential code to cooperate in glutamate synapse development. J Neurosci 30:7495–7506.

Small DH, Nurcombe V, Reed G, Clarris H, Moir R, Beyreuther K, Masters CL (1994) A heparin-binding domain in the amyloid protein precursor of Alzheimer's disease is involved in the regulation of neurite outgrowth. J Neurosci 14:2117–2127.

Smith PD, Coulson-Thomas VJ, Foscarin S, Kwok JC, Fawcett JW (2015) GAG-ing with the neuron: the role of glycosaminoglycan patterning in the central nervous system. Exp Neurol 274:100–114.

Stahl R, Schilling S, Soba P, Rupp C, Hartmann T, Wagner K, Merdes G, Eggert S, Kins S (2014) Shedding of APP limits its synaptogenic activity and cell adhesion properties. Front Cell Neurosci 8:410.

Sudhof TC (2017) Synaptic neurexin complexes: a molecular code for the logic of neural circuits. Cell 171:745–769.

Takahashi H, Arstikaitis P, Prasad T, Bartlett TE, Wang YT, Murphy TH, Craig AM (2011) Postsynaptic TrkC and presynaptic PTPσ function as a bidirectional excitatory synaptic organizing complex. Neuron 69:287–303.

Takahashi H, Katayama K, Sohya K, Miyamoto H, Prasad T, Matsumoto Y, Ota M, Yasuda H, Tsumoto T, Aruga J, Craig AM (2012) Selective control of inhibitory synapse development by Slitrk3-PTPδ trans-synaptic interaction. Nat Neurosci 15:389–398.

Uemura T, Lee SJ, Yasumura M, Takeuchi T, Yoshida T, Ra M, Taguchi R, Sakimura K, Mishina M (2010) Trans-synaptic interaction of GluRδ2 and Neurexin through Cbln1 mediates synapse formation in the cerebellum. Cell 141:1068–1079.

Wang Z, Wang B, Yang L, Guo Q, Aithmitti N, Songyang Z, Zheng H (2009) Presynaptic and postsynaptic interaction of the amyloid precursor protein promotes peripheral and central synaptogenesis. J Neurosci 29:10788–10801.

Yuzaki M, Aricescu AR (2017) A GluD coming-of-age story. Trends Neurosci 40:138–150.

Yuzaki M (2018) Two classes of secreted synaptic organizers in the central nervous system. Annu Rev Physiol 80:243–262.

Zhang P, Lu H, Piexoto RT, Pines MK, Ge Y, Oku S, Siddiqui TJ, Xie Y, Wu W, Archer-Hartmann S, Yoshida K, Tanaka KF, Aricescu AR, Azadi P, Gordon MD, Sabatini BL, Wong RO, Craig AM (2018) Heparan sulfate organizes neuronal synapses through neurexin partnerships. Cell 174: 1450–1464.e23.